

## NEUTRON SCATTERING STUDIES OF $n(p)$ AT REACTOR SOURCES

H. A. Mook

CONF-8810118--2

Oak Ridge National Laboratory  
Solid State Division  
Oak Ridge, TN 37831-6031

DE89 005127

What follows is an account of neutron scattering studies on liquid helium done at Oak Ridge over the last 15 or so years. As time progressed, the measurement techniques improved considerably, but more important was our improved understanding of the measurements. In particular, a better understanding was gained of the difficulty of obtaining a condensate fraction from measurements of  $S(Q, \omega)$  of liquid  ${}^4\text{He}$ .

The idea that  ${}^4\text{He}$  can undergo Bose Einstein condensation at low temperatures has generated great interest in much of the scientific community. It is not often one can observe the effects of quantum mechanics on a macroscopic scale. The idea behind the neutron scattering experiment to observe Bose Einstein condensation is extraordinary simple if one uses high enough neutron energies so that the impulse approximation correctly describes the scattering. The experiment is done as shown in Fig. 1 by bringing a mass 1 neutron with wave vector  $k_0$  and energy  $E_0$  incident on the mass 4 He and measuring the scattering at a fixed angle. If the He is at rest, one gets a peak in the scattering at an energy  $\hbar \omega$  that is given by the energy and momentum conservation relations for mass 4 and mass 1 particles. However, if the He is in motion in the liquid, sometimes it moves along the incident neutron path and sometimes opposite to it so that the neutron is Doppler shifted in the scattering process, and the scattering distribution is broadened. If one has a fraction of the atoms in the He that are at rest as they would be in the case of Bose Einstein condensation, then the scattering distribution would be a sharp peak on top of the broad distribution.

In considering an experiment, the first thing to think about is how wide the scattering distribution  $S(Q, \omega)$  is from the motion of the He atoms in the normal liquid. It turns out that the energy width in meV of the scattering distribution is nearly equal to the momentum transfer  $Q$  in  $\text{\AA}^{-1}$  at which the experiment is performed so that the width  $\Delta E$  (meV)  $\approx Q(\text{\AA}^{-1})$ . Hohenberg and Platzman<sup>1</sup> considered such a measurement and expressed the need for high energy neutrons, so let us first consider the case for  $Q = 100 \text{\AA}^{-1}$ .

NEUTRON

8

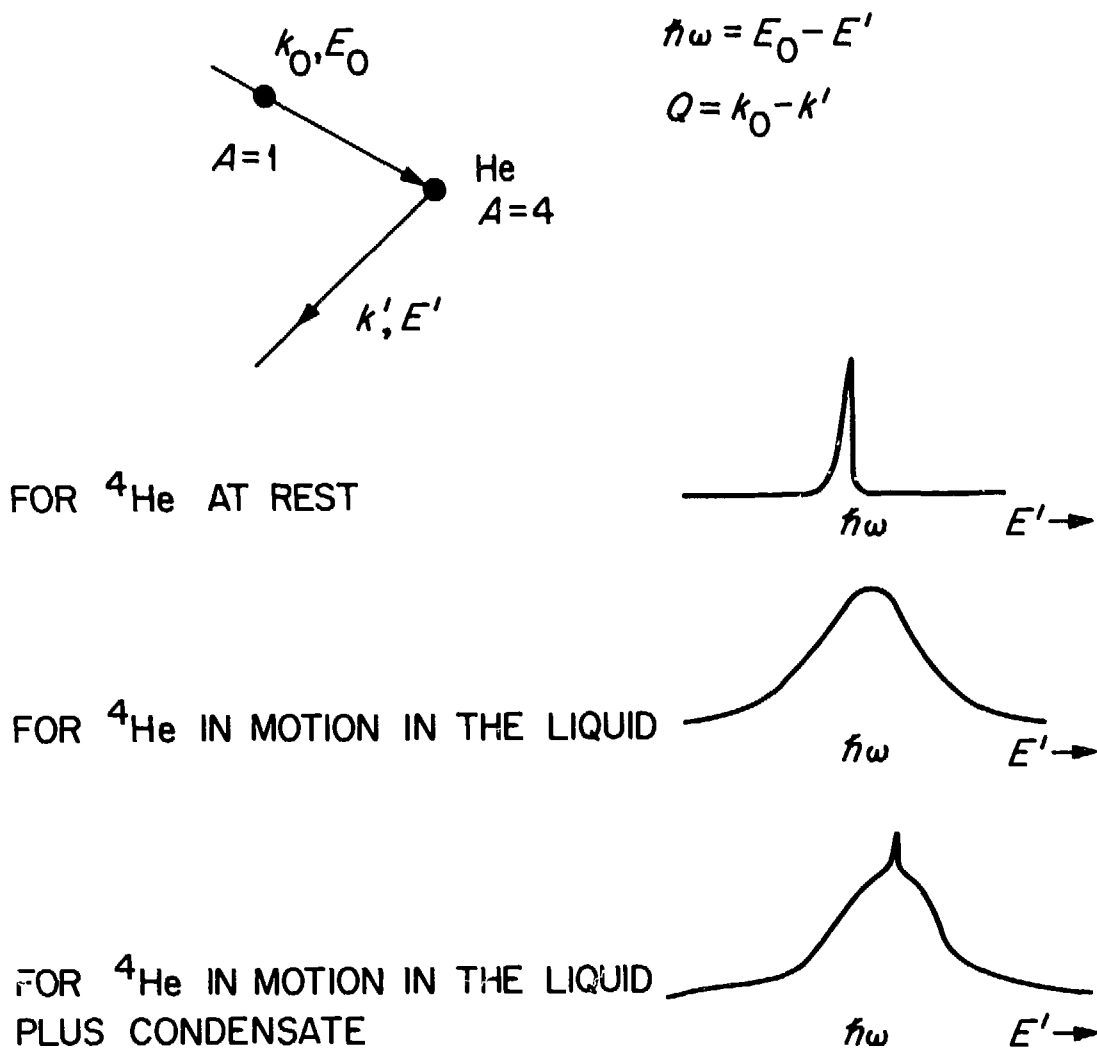


Fig. 1 Neutron scattering pattern for  ${}^4\text{He}$  that has undergone Bose Einstein Condensation.

For a momentum transfer of  $100\text{\AA}^{-1}$ , we need incident neutrons of momentum about  $100\text{\AA}^{-1}$  or 20.75 eV in energy. The fractional energy resolution desired is roughly given by

$$\frac{0.1 \text{ eV (width in meV)}}{20.75 \text{ eV}} = 0.0048.$$

We really should have five resolution elements across the peak in order to see anything interesting which means we not only have to do the experiment with 20 eV neutrons, but we need resolutions on the order of 0.1%. This is an exceedingly difficult, if not impossible, prospect; so let us consider an easier experiment and try a  $Q$  of  $15\text{\AA}^{-1}$ .

For a momentum transfer of  $15\text{\AA}^{-1}$ , we need incident neutrons of momentum about  $15\text{\AA}^{-1}$  which is 460 meV in energy.

$$\frac{15(\text{width in meV})}{460\text{meV}} = 0.032.$$

Divide this by five to get five resolution elements, and we have resolutions of somewhat under 1%. We can get 460 meV neutrons from reactor sources, and the resolution is difficult but possible to achieve. In 1971, such an experiment was undertaken<sup>2</sup> using a triple-axis spectrometer at the High Flux Isotope Reactor (HFIR); the results are shown in Fig. 2. Data were taken at 1.2K and 4.2K and the resolution is indeed such that about five resolution elements are across the peak. This is really quite an extraordinary experiment as the counting time was on the order of six months, far longer than it would be possible to count today because of the demand for beam time on the instruments. Rather good statistics were collected in the neighborhood of the peak where the condensate should be visible, while less precise data were collected in the wings of the distribution.

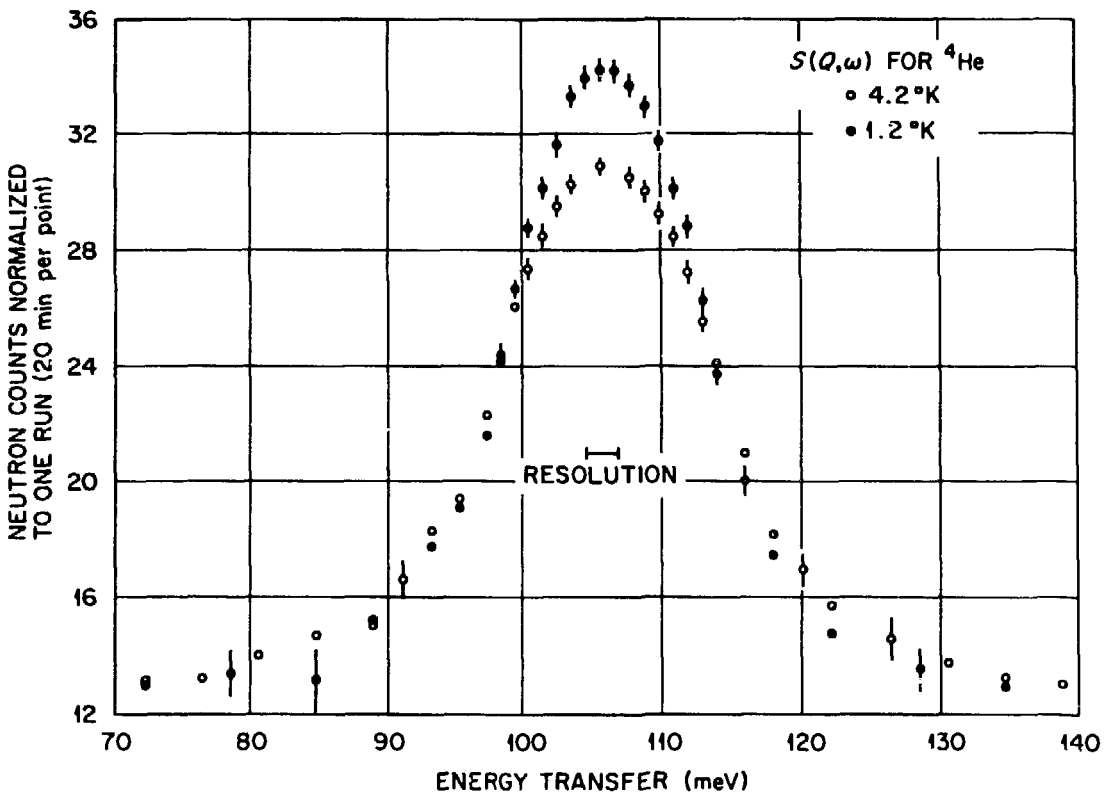


Fig. 2 Triple-axis measurement of  $S(Q, \omega)$  for  $^4\text{He}$  at 4.2K and 1.2K.

It is obvious that no sharp condensate peak is visible on  $S(Q,\omega)$  measured at 1.2K, and indeed, as we know now, no sharp peak is expected even for momentum transfers two or three times this value. We were then left with the problem of extracting a condensate fraction. With the idea that  $S(Q,\omega)$  at 1.2K should consist of two distributions, the 4.2K and the 1.2K data were least-squares fitted with two distributions. It turned out that the 4.2K data were well fitted using one distribution, but the fit only gave good results with two distributions for the 1.2K data. Assuming that the smaller of the distributions stemmed from the condensate, a condensate fraction of about 2.5% was determined. It turns out that this is not a good way to extract a condensate fraction as it ignores the change in  $S(Q,\omega)$  in going from 4.2K to 1.2K, except for the very top of the peak. In the paper it was pointed out that if one considers the area between two distributions, a condensate fraction of about 10% is indicated, and it turns out that this is a better way to analyze the data.

A real breakthrough came though with the papers of Martel et al.,<sup>3</sup> Woods and Sears,<sup>4</sup> and Sears, Svensson, Martel, and Woods<sup>5</sup> who outlined a way to deal with data like that shown above. Their method relied on symmetrizing the data about the calculated recoil energy to minimize final

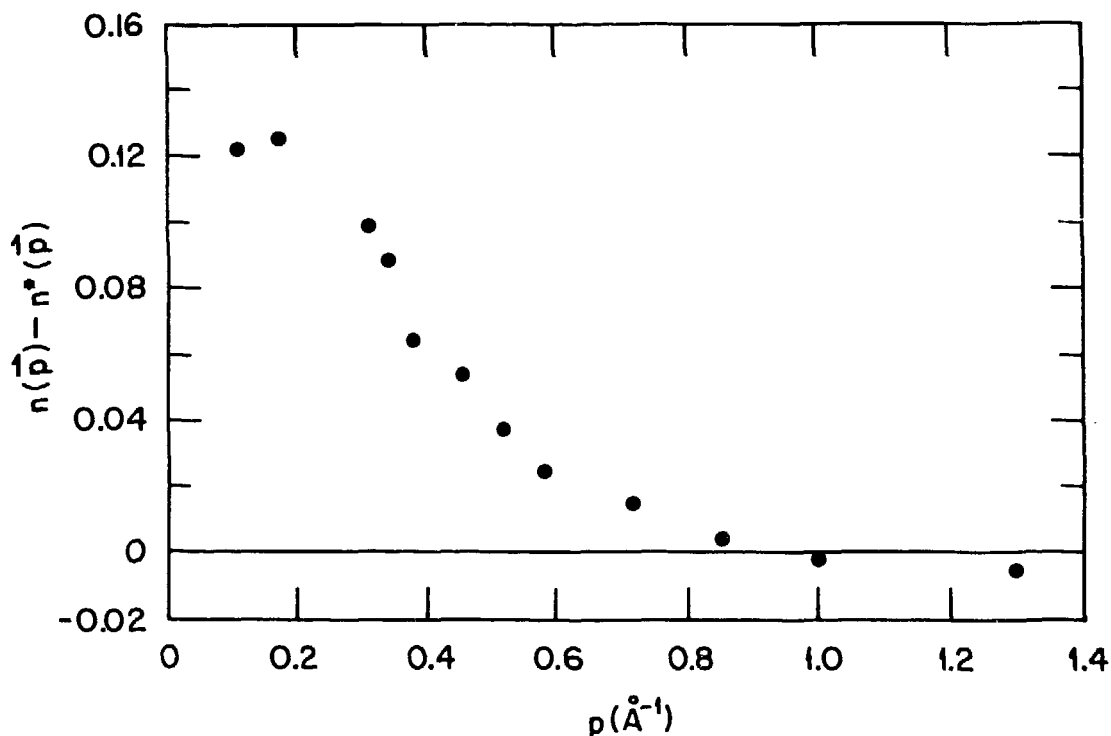


Fig. 3  $n(p)$  at 1.2K minus  $n(p)$  at 4.2K for the triple-axis data shown in Fig. 1.

state effects, and if low Q data are used, to average data together at a number of Q values. The momentum distributions  $n(p)$  were then obtained from the data, and the condensate fraction determined from the formalism given by

$$n_0 = \frac{\epsilon}{1 - \beta + \gamma} \quad (1)$$

where

$$\epsilon = \int_0^{p_c} [n(p) - n^*(p)] p^2 dp \quad (2)$$

and

$$\beta = \int_0^{p_c} p^2 dp \quad (3)$$

where  $p_c$  is the point where  $n(p) - n^*(p)$  becomes negative and  $\gamma$  is a correction term that becomes large near the  $\lambda$  temperature. Fig. 3 shows the quantity  $n(p) - n^*(p)$  needed in obtaining the condensate fraction. We note that the result is fairly accurate, but that little information is available beyond  $1 \text{ \AA}^{-1}$ , as high quality data were only taken near the top of the distribution. Using the value for  $\gamma$  given in Ref. 5, a condensate fraction is obtained of about 10%.<sup>6</sup> However, it should be noted that Griffin<sup>7</sup> has recalculated  $\gamma$ , and a smaller condensate fraction would be obtained using his values.

It would clearly be of interest to obtain good measurements of  $n(p)$  over a reasonably complete  $p$  range, but to do so is difficult on triple-axis spectrometers because of the long counting times. The experiment is easier with time-of-flight since the energy resolution can be uncoupled from the Q resolution in this technique, and high Q resolution is not needed. A time-of-flight spectrometer was developed that could make fast neutron pulses by ultrasonic techniques. As shown in Fig. 4, Bragg reflection takes place from a perfect crystal according to the relation  $\lambda = 2d \sin \theta$ ; a very narrow range of  $\theta$  corresponds to a narrow range of  $\lambda$ , and little scattering intensity is obtained. If a high intensity ultrasonic pulse is incident on a transducer attached to the crystal, a band of  $\lambda$ 's is obtained from each  $\theta$ , and a large neutron pulse is achieved. Since the pulse is electronic, it can be repeated at any time in a precise manner. This makes it possible to use the correlation technique, as shown in Fig. 5. In a normal chopper, a pulse is made and the neutrons are counted from this pulse over some time  $\tau$  long compared to the pulse. With the correlation technique, a signal function  $S(t)$  is made incident on the sample, and a convolution of the signal function and the function you wish to obtain,  $F(t)$ , is counted. However,  $S(t)$  can be constructed so that  $F(t)$  can be obtained easily by the cross correlation of the counted neutrons,  $Z(t)$ , with the signal function. For a continuous source, a much improved duty cycle can be obtained that can be 50% in an ideal case. For He, the gain is less, but is appreciable, especially for  $^3\text{He}$  which has a very high neutron absorption cross section.

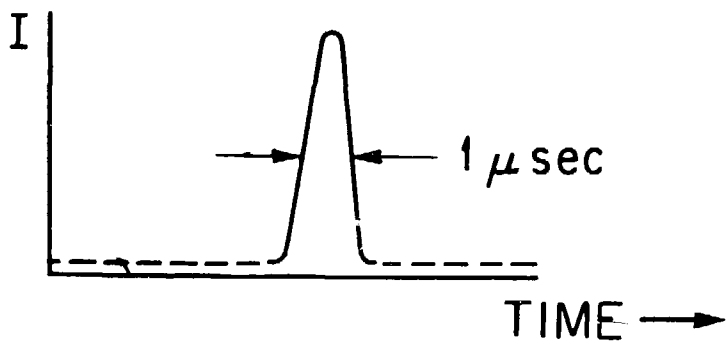
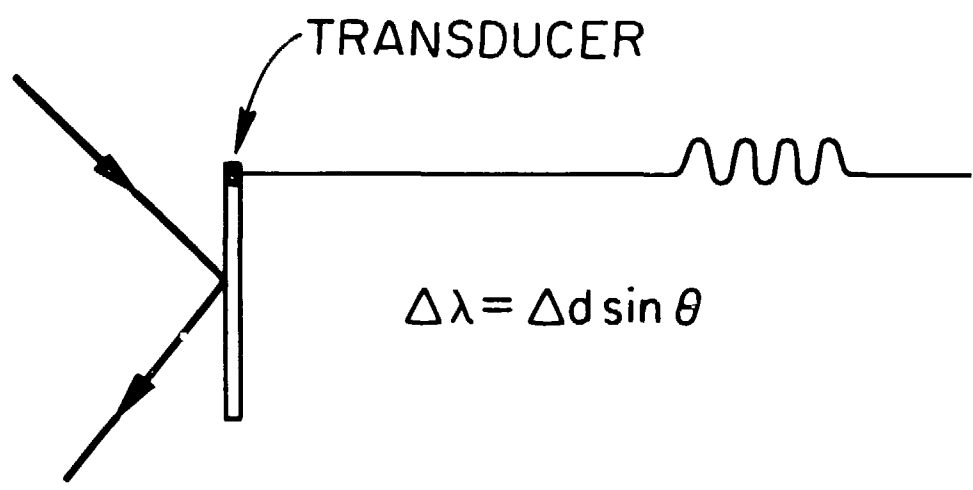
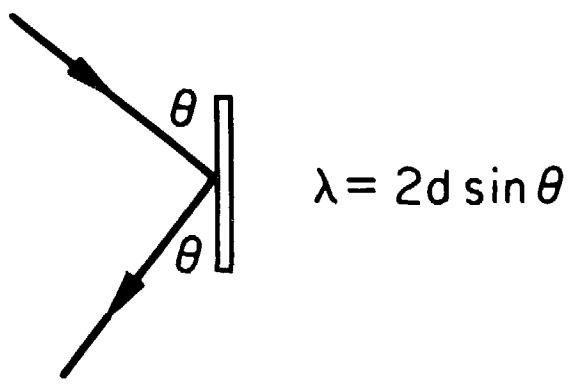
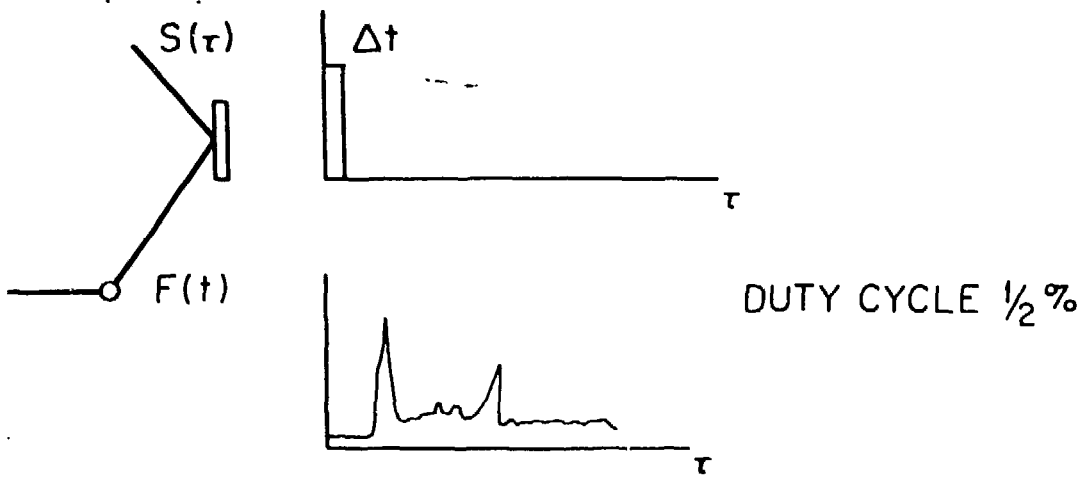


Fig. 4 Production of high intensity short time neutron pulses by ultrasonic techniques.



WITH CROSS CORRELATION TECHNIQUE



$S(t)$  CONSTRUCTED SO THAT

$$\sum_{\tau} S(\tau) S(t+\tau) = \begin{cases} 1 & t=0 \\ 0 & t \neq 0 \end{cases}$$

$$Z(t+\tau) = \sum_{\tau} S(t+\tau) F(t)$$

BUT

$$F(t) = \sum_{\tau} S(\tau) Z(t+\tau) \quad \text{DUTY CYCLE } 50\%$$

Fig. 5. The neutron cross correlation time-of-flight technique can give a high duty cycle for steady state sources.

A problem with the cross correlation technique is that the pulse must be of an exact shape or else distortions of the desired  $F(t)$  spectrum are obtained. This shape cannot be made perfectly by any technique including the ultrasonic one. However, one can correct for this by measuring the signal function that is actually generated and constructing a new function to use in the cross correlation that removes the distortions in the correlated data. The cross correlation is given by

$$F_j = \sum_i^N Z_i S_{i+j} \quad (4)$$

which can be written in matrix form as

$$F = ZS \quad (5)$$

where S is an N by N circulant matrix with elements  $a_{ij} = a_{i-j}$ . If the signal function as measured by a detector is given by Z, and P is the ideal shape desired in the cross correlation, one can solve for a matrix  $\tilde{S}$  by

$$Z\tilde{S} = P \quad (6)$$

The matrix  $\tilde{S}$  is then used to cross correlate the measured data and corrects all errors for improper pulse shape. It turns out that the ideal pulse shape can be of any width so that choosing a narrow shape automatically deconvolutes the resolution from the data. Of course the statistical accuracy is decreased if a narrow width is chosen, but one is free to choose the best trade off between resolution and statistical accuracy.

The next step is to determine how to find  $n(p)$  from data taken at constant angle and not at constant Q. The cross section for scattering in the impulse approximation is given by

$$\begin{aligned} \frac{d^2\sigma}{d\Omega d\omega} &= c \frac{k_f}{k_i} S(Q, \omega) \\ &= c \frac{k_f}{k_i} \sum_p n_p \delta\left(\omega - \frac{Q^2}{2m} - \vec{Q} \cdot \frac{\vec{p}}{m}\right), \end{aligned} \quad (7)$$

where c is a constant,  $k_f$  and  $k_i$  are the final and incident neutron wave vectors, p is the momentum of the helium atom before the scattering event, m is the  $^4\text{He}$  mass, and  $\hbar$  has been set equal to 1.

For constant Q,

$$\rho n_p|_{p_{\min}} = (4 \pi Q^2 \rho / m^2) \partial S(Q, \omega) / \partial \omega, \quad (8)$$

where  $\rho$  is the density and

$$p_{\min} = [\omega - \omega(Q)](Q/m)^{-1},$$

with  $\omega(Q)$  the neutron energy transfer for the momentum Q. While for constant angle,



$$\rho n_p |_{\rho_{\min}} = \frac{\pi^2 \rho}{cm} \left(1 - \frac{\omega}{\epsilon_i}\right)^{-1/2} \left\{ 8 \omega(Q) \frac{\partial}{\partial \omega} + \left[ \frac{4 \omega(Q)}{\epsilon_i - \omega} - 1 + \left(1 - \frac{\omega}{\epsilon_i}\right)^{-1/2} \cos \theta \right] \right\} \frac{d^2 \sigma}{d\Omega d\omega} \\ \times \left\{ 1 + \frac{1}{8} \left(1 + \frac{\omega}{\omega(Q)}\right) \left[ 1 - \left(1 - \frac{\omega}{\epsilon_i}\right)^{-1/2} \cos \theta \right] \right\}^{-1} \quad (9)$$

where  $\epsilon_i$  is the incident neutron energy, and  $\theta$  is the scattering angle.

With the cross correlation neutron time-of-flight operational, it was then possible to measure  $n(p)$  with good resolution in a reasonable amount of time. An experiment was performed with a  $Q$  of  $14.79 \text{ \AA}^{-1}$  and  $n(p)$  obtained from the measured  $S(Q, \omega)$  using Equation 9.<sup>8</sup> A plot of  $\rho n(p)$  is shown in Fig. 6 compared with a calculation by Kalos.<sup>9</sup> There appears to be a peak at low  $p$  in  $\rho n(p)$ , but within the statistical error shown it probably more accurate to say that there is extra scattering at low  $p$  that is indicative of the condensate. Using similar data taken above the  $\lambda$  point and calculating the condensate fraction by Equation 1, a condensate fraction of about 12% is obtained. Within the measured errors and neglecting the extra scattering at low  $p$  that comes from the condensate, the measured and calculated  $\rho n(p)$  distributions are in good agreement.

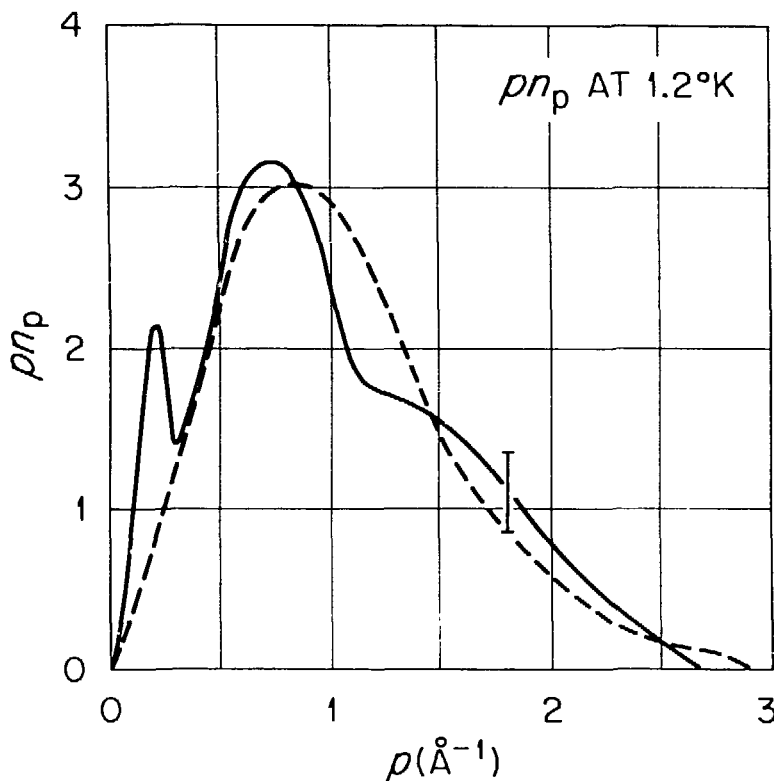


Fig. 6  $\rho n_p$  for  $^4\text{He}$  at 1.2K. The solid line is a calculation by Kalos.

At this time, substantial improvements were made to the spectrometer. First, a large crystal in conjunction with a convergent slit was used to pulse the beam, as shown in Fig. 7. The crystal was placed in such a way that the longer wavelength, or lower energy neutrons, were reflected from a place on the crystal nearer the sample so that they arrived at the detector at the same time as the faster neutrons that started farther away from the sample. This meant that a much bigger wavelength spread could be used resulting in much higher intensity without increasing the energy resolution. Also, additional pulsing crystals were used, as shown on the bottom of Fig. 7, permitting an even bigger wavelength spread. It is only necessary to delay the pulse chain to each crystal by the proper amount so that all neutrons arrive at the detector at the same time. Also, at this time, more detectors were added to the spectrometer giving 32 separate detector banks of 5 detectors each. This makes it possible to take data at 32 separate Q values simultaneously.

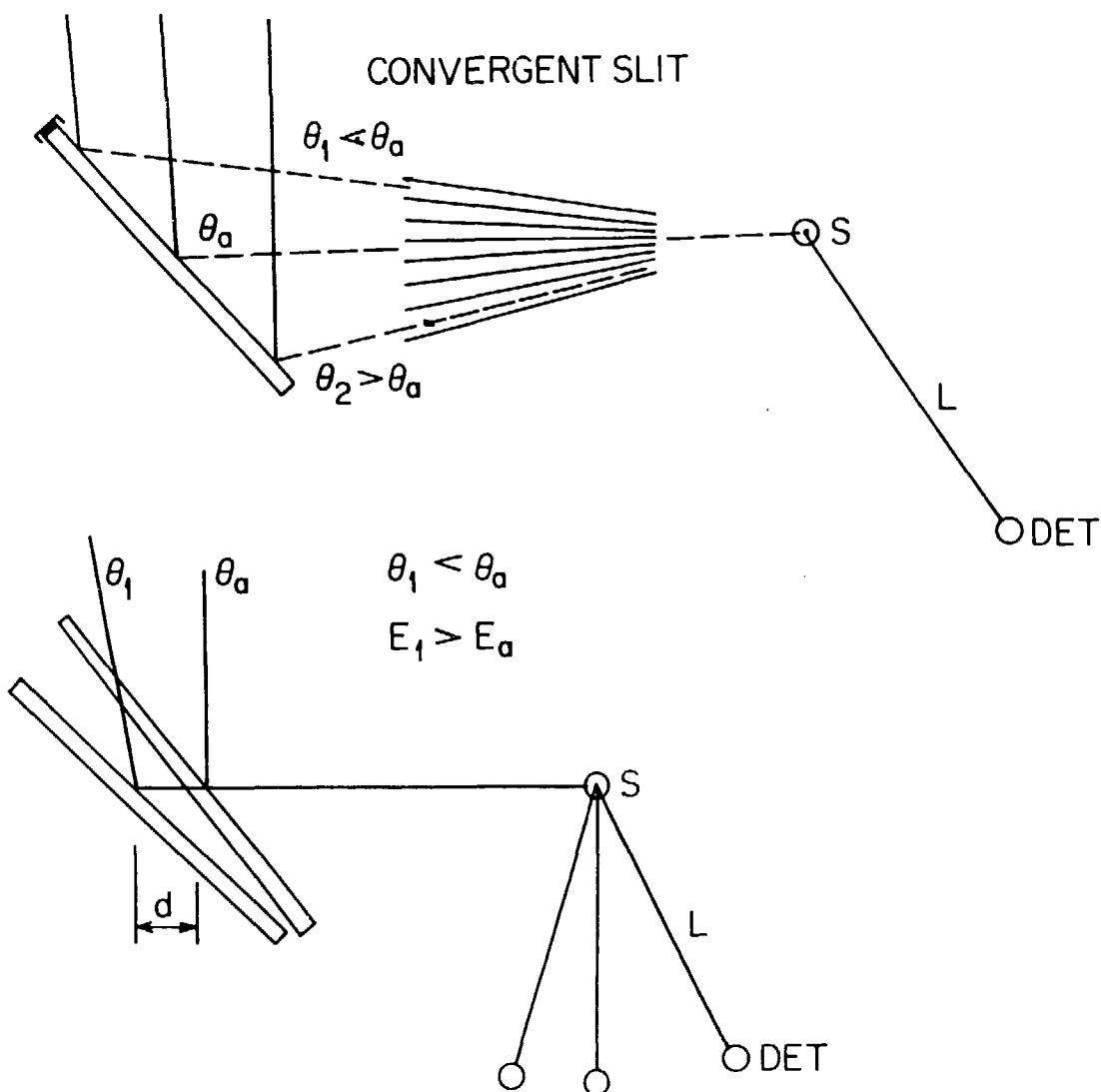


Fig. 7 A convergent slit and multiple pulsing crystals can greatly increase the neutron intensity if the pulse timing is such that all neutrons reach the detector at the same time.

With these improvements, it became possible to measure  $S(Q, \omega)$  for  ${}^4\text{He}$  with good resolution at 32 separate  $Q$  values at reasonable counting rates. Figure 8 shows measurements of  $n(p) - n^*(p)$  for three temperatures.  $n(p)$  was obtained by symmetrizing  $S(Q, \omega)$  at a number of  $Q$ 's and adding the calculated momentum distributions. A condensate fraction of about 10% was obtained at the lowest temperature<sup>10</sup> in good agreement with other results.

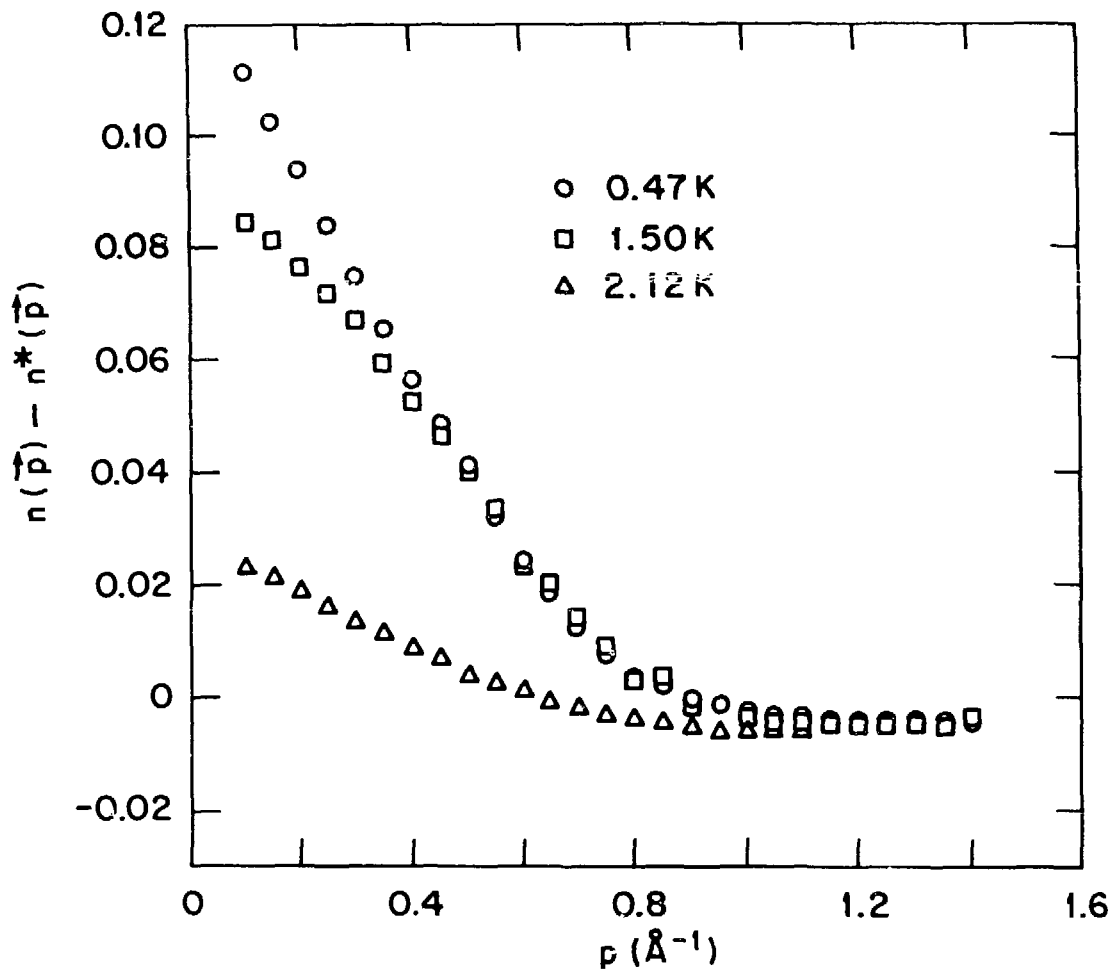


Fig. 8  $n(p)$  for  ${}^4\text{He}$  at low temperatures minus  $n^*(p)$ , the momentum distribution measured just above the  $\lambda$  point.

The spectrometer improvements made it possible to perform detailed measurements on  $^3\text{He}$  for the first time.<sup>11</sup>  $^3\text{He}$  has an absorption cross section for neutrons of about 10,000 barns, making the measurements very difficult, so of course the data obtained is not nearly as good as with  $^4\text{He}$ . Measurements were first made at a temperature of 1.2K which is too high to observe any Fermi-liquid effects. In this case,  $S(Q,\omega)$  should be nearly Gaussian, and Fig. 9 shows one of the measurements for a scattering angle of  $81.6^\circ$ . The solid line is a least squares fit to two Gaussians, one centered at energy transfer zero stemming from the sample container, and the other from the  $^3\text{He}$ . From data like these, the peak widths and positions were determined. The top of Fig. 10 shows the width divided by  $Q$  as a function of  $Q$ . Oscillations in this curve have been found for  $^4\text{He}$  that can be traced back to the oscillations in the  $^4\text{He}$ - $^4\text{He}$  scattering cross section. The curve for  $^3\text{He}$  looks like it may have a dip in it at a  $Q$  of around  $5.5\text{\AA}^{-1}$  although the statistics are probably not inconsistent with a straight line. The minimum for  $^4\text{He}$  occurs at  $4.5\text{\AA}^{-1}$  and this is certainly not observed. A more accurate experiment is needed, but the indications are that the width oscillations are different for  $^3\text{He}$  than for  $^4\text{He}$ , as might be expected, since the oscillations in the atomic scattering cross sections are different in the two materials.

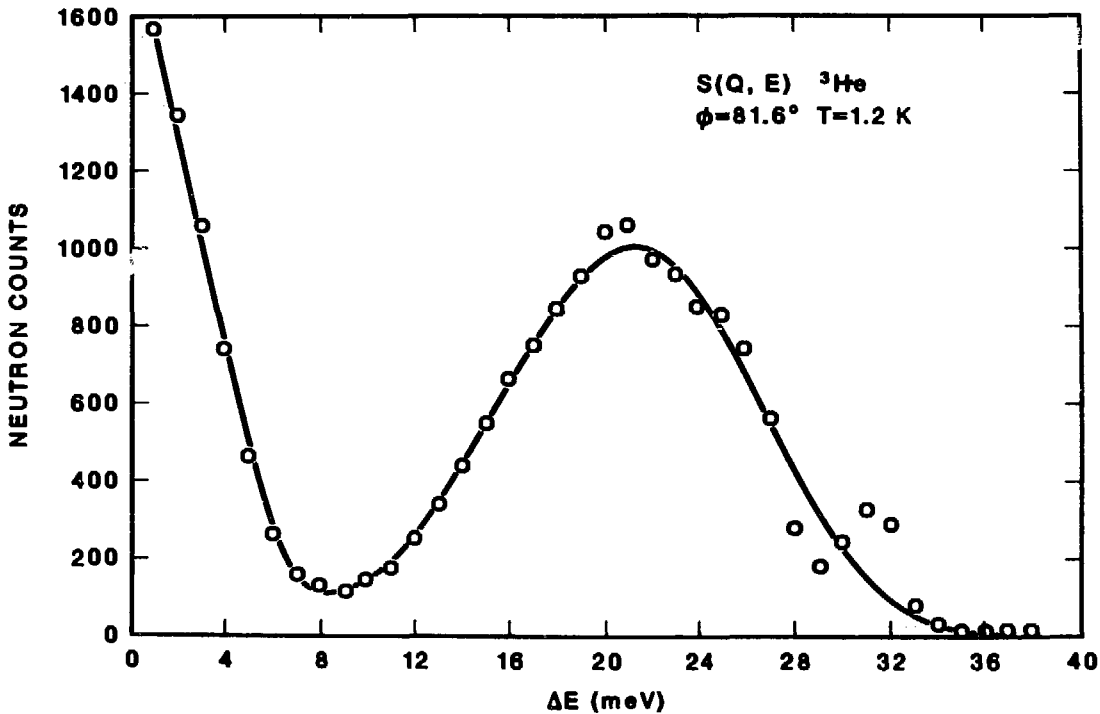


Fig. 9  $S(Q,\omega)$  for  $^3\text{He}$  at 1.2K for the detector bank at  $81.6^\circ$ .

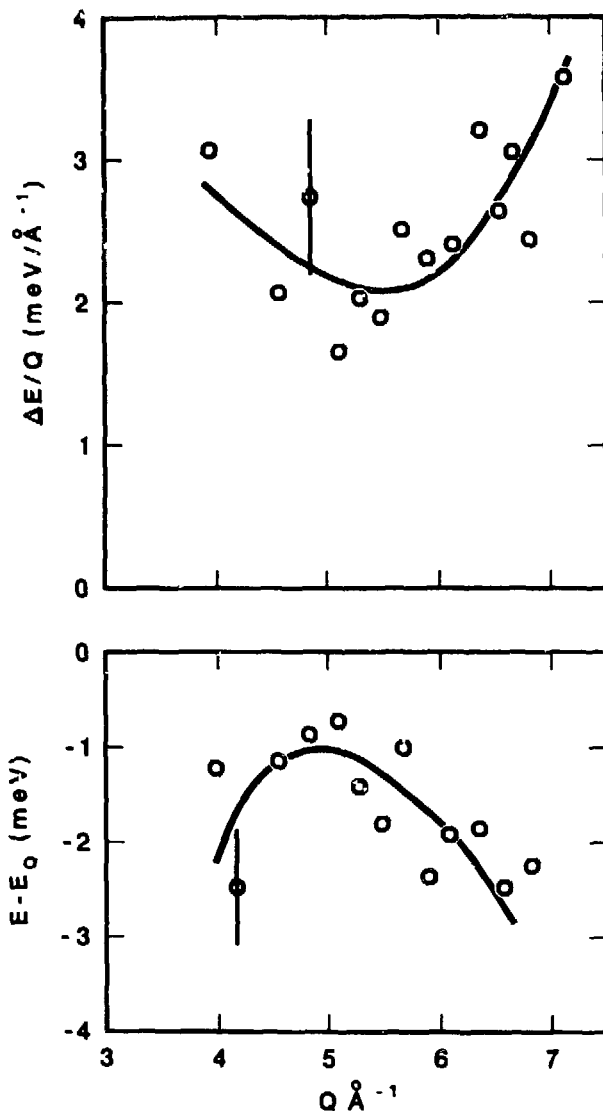


Fig. 10 Measurements of the relative width and position of  $S(Q, \omega)$  for  $^3\text{He}$  at 1.2K as a function of  $Q$ .

The bottom of Fig. 10 shows the energy difference between the observed peaks in  $S(Q, \omega)$  and the calculated position given by the impulse approximation. This difference is a maximum at  $4.5 \text{ \AA}^{-1}$  for  $^4\text{He}$  but appears to be near a minimum for  $^3\text{He}$ . It again would be desirable to do a more accurate experiment, but it appears that if there are oscillations in the positions of the  $S(Q, \omega)$  distributions as a function of  $Q$  for  $^3\text{He}$ , the oscillations have a different phase than they do for  $^4\text{He}$ .

The most interesting effects in  $^3\text{He}$  occur at low temperatures where the material is thought to have properties that can be described in terms of a Fermi-liquid. The sample of  $^3\text{He}$  was cooled to 0.37K, which was the low temperature limit of the experiment, and  $S(Q,\omega)$  determined for 32 different  $Q$  values.  $n(p)$  was then determined by symmetrizing the  $S(Q,\omega)$  data and averaging the results for different  $Q$  values as was done earlier for  $^4\text{He}$ . The result is shown in Fig. 11. The solid line is a least squares fit by an ideal Fermi-gas distribution for  $T_F = 1.8\text{K}$ . Again, because of the difficulty of the experiment, the error bars are larger than would be desirable. The Fermi surface is not expected to be sharp because of broadening by temperature and final state effects. Further experiments should be done at a lower temperature so that the final state effects can be isolated. Nevertheless, the experiment gives a result for the Fermi temperature that is in good agreement with generally accepted values.

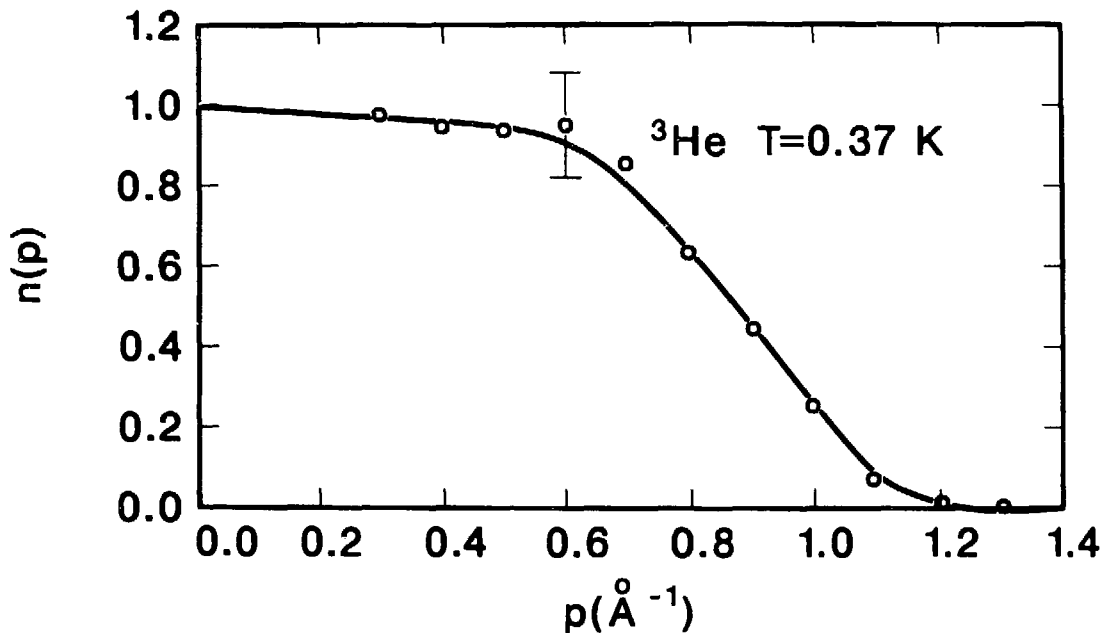


Fig. 11  $n(p)$  for  $^3\text{He}$  at 0.37K.

We see then that we have come a long way in the last 15 years in our ability to produce reliable neutron scattering results for the quantum liquids  $^4\text{He}$  and  $^3\text{He}$ . Part of that gain, particularly for  $^3\text{He}$ , has been the substantial improvement in instrumentation. A very important factor in the determination of the Bose condensate has been a better understanding of how to analyze the data. Probably more work needs to be done on this, but at least an analysis procedure now exists that gives consistent results for a wide variety of measurements. Measurements are only beginning on  $^3\text{He}$ , but at least they appear to be possible. Certainly we can look forward to much better results in the next few years. Finally, it is very important to be able to evaluate the effects of final state effects on the measurements. It is obvious that a lot of progress has been made in this regard, but it is equally obvious that more remains to be done.

This research was supported by the Division of Materials Sciences, U.S. Department of Energy under Contract No. DE-AC05-84OR21400 with Martin Marietta Energy Systems, Inc.

## References

1. P. C. Hohenberg and P. M. Platzman, *Phys. Rev.* **192**, 198 (1966).
2. H. A. Mook, R. Scherm, and M. K. Wilkinson, *Phys. Rev. A* **6**, 2268 (1972).
3. P. Martel, E. C. Svensson, A. D. B. Woods, V. F. Sears, and R. A. Cowley, *J. Low Temp. Phys.* **23**, 285 (1976).
4. A. D. B. Woods and V. F. Sears, *Phys. Rev. Lett.* **39**, 415 (1977).
5. V. F. Sears, E. C. Svensson, P. Martel, and A. D. B. Woods, *Phys. Rev. Lett.* **49**, 279 (1982).
6. H. A. Mook, *Phys. Rev. B* **37**, 5806 (1988).
7. A. Griffin, *Phys. Rev. B* **32**, 3289 (1985).
8. H. A. Mook, *Phys. Rev. Lett.* **32**, 1167 (1974).
9. M. H. Kalos (private communication).
10. H. A. Mook, *Phys. Rev. Lett.* **51**, 1454 (1983).
11. H. A. Mook, *Phys. Rev. Lett.* **55**, 2452 (1985).

## DISCLAIMER

This report was prepared as an account of work sponsored by an agency of the United States Government. Neither the United States Government nor any agency thereof, nor any of their employees, makes any warranty, express or implied, or assumes any legal liability or responsibility for the accuracy, completeness, or usefulness of any information, apparatus, product, or process disclosed, or represents that its use would not infringe privately owned rights. Reference herein to any specific commercial product, process, or service by trade name, trademark, manufacturer, or otherwise does not necessarily constitute or imply its endorsement, recommendation, or favoring by the United States Government or any agency thereof. The views and opinions of authors expressed herein do not necessarily state or reflect those of the United States Government or any agency thereof.